Pak. J. Bot., 54(6): 2033-2042, 2022. DOI: http://dx.doi.org/10.30848/PJB2022-6(15)

RHODODENDRON MICRANTHUM RmMDH GENE ENCODING MALIC DEHYDROGENASE CONFERS TOLERANCE TO ABIOTIC STRESS IN TRANSGENIC *NICOTIANA TABACUM*

SHAN-JUN YI[1], WEI LI[2,*], ZHEN-YUAN SUN[3], XIAO-XING ZHOU[4] AND XIAO-PING LI[5]

[1]*Planning and Design Institute of Forest Products Industry, National Forestry and Grassland Administration, Beijing 100010, China*
[2]*College of Landscape Architecture and Forestry, Qingdao Agricultural University, Qingdao 266000, China*
[3]*State Key Laboratory of Forest Genetic and Tree Breeding, Chinese Academy of Forestry, Beijing 100091, China*
[4]*Academy of Agricultural Planning and Engineering, Ministry of Agriculture and Rural Affairs, Beijing 100125, China*
[5]*Bei Jing He Ping Li Hospital, Beijing, 100013, China*
[*]*Corresponding author's email: lwcsu_caf@163.com*

Abstract

Malic dehydrogenases (MDHs) have vital functions in the development of plants. In this study, the full-length coding sequence of *RmMDH* (GenBank ID: JQ412742) was isolated from *Rhododendron micranthum* Turcz. *RmMDH* had a 999-bp open reading frame (ORF), which was responsible for encoding a protein that contained 332 amino acid residues, its theoretical isoelectric point was 6.40 and its predicted molecular mass was 35.61 kDa. RmMDH was predicted to localize to the chloroplast. Real-time RT-PCR analyses showed that the transcript levels of *RmMDH* in *Rh. Micranthum* differed among tissues (highest levels in the flowers, lowest levels in the roots) and developmental stages (highest transcript levels in flowers at the full-bloom stage, and in leaves in October). *RmMDH* was introduced into tobacco, and its integration into the genome was confirmed by PCR and Southern blot analyses. Compared with wild-type tobacco, transgenic plants showed smaller leaves, shorter height, lower malondialdehyde contents, and higher proline contents. Transgenic plants showed stronger tolerance to NaCl, $NaHCO_3$, polyethylene glycol, and aluminum stresses relative to wild-type tobacco. Our results show that *RmMDH* dramatically affects plant growth and is involved in abiotic stress resistance. These results lay the foundation for the genetic improvement of *Rh. micranthum*.

Key words: *Rhododendron micranthum* Turcz; Malic dehydrogenase; *RmMDH*; Gene expression; Transgenic tobacco; Abiotic stress.

Introduction

Malic dehydrogenases (MDH) are widely distributed in plants, animals, and microorganisms, and are highly conserved. In plants, the availability of NAD(P)H affects the activity of MDHs, which catalyze the mutual transformation of malic acid and oxaloacetic acid (OAA) (Selinski *et al*., 2014). According to their subcellular location, plant MDHs can be divided into mitochondrial MDHs, peroxisome MDHs, plastid MDHs, and cytoplasmic MDHs (Gietl, 1992). These enzymes are involved in many physiological activities, including seed germination, plant growth, pollen development, fruit development, and stress resistance (Yao *et al*., 2011a; Yao *et al*., 2011b; Beeler *et al*., 2014; Rudrappa *et al*., 2008). Nine MDHs, including two peroxisome MDHs, are found from *Arabidopsis thaliana* (Pracharoenwattana *et al.*, 2007).

Malic acid has an important function in the response to abiotic stress, metabolism and nutrition of plant, which also accounts for a key intermediate produced in the tricarboxylic acid cycle (Schulze *et al*., 2002a; Schulze *et al*., 2002b; Scheibe, 2004). The high *MDH* transcript level is suggested previously to be related to the increased contents of malic acid. This may increase the osmotic pressure of cells, and/or increase the chelation and removal of aluminum ions to improve plants' tolerance to aluminum. Many studies have explored the complex functions of MDHs. *MDH* gene expression is reported in certain articles to improve plants' tolerance to aluminum. For instance, in *Medicago sativa*, the cytoplasmic *MDH* overexpression increased the organic acid exudation rate from root by 4 folds, compared with that of wild type. This improved tolerance to Al^{3+} by chelating aluminum ions in the soil (Tesfaye *et al*., 2001). Overexpression of *MDH* genes encoding plastid and cytoplasmic-soluble MDHs from *A. thaliana* improved the tolerance of transgenic tomato to aluminum (Zhang, 2008; Wang *et al*., 2010). Overexpression of *MDH* improved the tolerance of alfalfa to aluminum toxicity in acid soil (Luo *et al*., 2004), and overexpression of an *MDH* from *A. thaliana* in tobacco improved its tolerance to aluminum (Wang *et al*., 2010). Transgenic tobacco plants expressing an *MDH* from orange also showed improved aluminum tolerance (Zhang, 2008). In the transgenic tobacco, *MDHs* overexpression in *Escherichia coli* and *A. thaliana* were shown to promote the synthesis of malic acid and improve aluminum resistance (Wang *et al*., 2010). Further studies have shown that *MDH* expression responds to abscisic acid (ABA), low temperature, and salt stresses, indicating the key functions of MDHs in enhancing the abiotic stress resistance of plants. An apple *MDH* gene encoding a cytoplasmic MDH promoted the accumulation of malic acid in callus of transgenic apple and transgenic tomato by regulating gene levels associated with malic acid transport and decomposition, TCA cycle and gluconeogenesis (Yao *et al*., 2011b). This led to changes in the contents of certain substances, which increased the stress resistance of the transgenic materials.

There are many MDH isomers. Some MDH subtypes in plants exhibit special subcellular locations, which also interact with different coenzymes. Many MDH subtypes are discovered from diverse species (Yao *et al*., 2011b; Abd *et al*., 2015; Zhang *et al*., 2015). Therefore, it is

unknown whether MDHs of one species will have the same activity or effect when expressed in another species.

Rh. micranthum Turcz is a semi evergreen shrub with a high ornamental and medicinal value. However, it has strict growth requirements. It grows best in loose-textured acid soil that is rich in humus, and it does not tolerate hot, dry, and saline alkali soil. The soil in most areas of northern China is alkaline, so *Rh. Micranthum* introduced to these areas grows poorly or does not survive. Many researchers have attempted to develop methods to introduce and cultivate acid-loving *Rhododendron* in an alkaline environment. At present, acidic substances are applied to soil to reduce its alkalinity, but this is a temporary fix. Consequently, the introduction and cultivation of *Rh. micranthum* into areas with alkaline soil have not been successful. The introduction of exogenous genes into target species using modern genetic engineering methods can not only achieve directional improvement, but also save costs and improve breeding efficiency. Many previous studies have explored the functions of *MDH* genes, but most have focused on model plants and crops (Gietl 1992; Pracharoenwattana *et al*., 2007; Tomaz *et al*., 2010; Selinski *et al*., 2014). The roles of *MDH* genes in ornamental plants such as *Rh. micranthum* are still unclear. It is possible that *MDH* overexpression could improve tolerance to salt, alkali, and aluminum in *Rh. micranthum*, but its *MDH* genes have not been cloned or functionally analyzed.

Therefore, in this study, we identified and cloned an *MDH* gene, designated as *RmMDH*, from *Rh. micranthum.* We analyzed its transcript levels different organs and tissues, and in leaves and flowers at different stages of development. We then studied its role in stress resistance and aluminum tolerance by overexpression in tobacco and *Rh. micranthum*.

Material and Methods

Sample collection and stress treatments: All tested samples (roots, stems, leaves, and flowers) were harvested from a 20-year-old *Rh. micranthum* tree growing at the Beijing Botanical Garden, Chinese Academy of Sciences. Leaf, root, and stem materials were collected in 2017 (from April to October). In the same year, flower tissues were collected at four developmental stages from 6 May to 6 July. Each test specimen was frozen within the liquid nitrogen at once and preserved under −80°C before to RNA isolation. To analyze the stress tolerance, seedlings with the age of 4 weeks were placed into Murashige and Skoog (MS) medium that contained 50 μM $AlCl_3$, 200 mM NaCl, 5% PEG 6000, or 20 mM $NaHCO_3$, and grown for 7 days.

Cloning of full-length *RmMDH* cDNA: The modified CTAB method was utilized to extract total RNA in the leaf samples of *Rh. micranthum* (Allen *et al*., 2006), in line with specific protocols. Later, SMART™ RACE cDNA Amplification Kit (Takara, Dalian, China) was employed to purify RNA and synthesize first-strand cDNA. Thereafter, this study cloned *RmMDH* full-length cDNA sequence based on the leaf samples of *Rh. micranthum* through rapid-amplification of cDNA ends (RACE). For RACE, the 3′ RACE primer (forward) along with 5′ RACE primer (reverse) supplemented in SMART™ RACE cDNA Amplification Kit (Clontech, Palo Alto, CA, USA) was adopted. According to 3′- and 5′-end sequences, this study synthesized the same primers for amplifying the *RmMDH* full-length sequence (Table 1). After gel purification, this study cloned PCR products to pMD19-T vector (Takara). Later, Sangon Biotech (Shanghai, China) was responsible for sequencing positive clones. Sequence of gene *RmMDH* was imported into GenBank (accession no JQ412742).

Table 1. Primers used in this study.

Primer name	Primer sequence (5' to 3')
3′-RACE-F	5′- CAGCGTGGTGCGGCTATTATCAAGGC-3′
5′-RACE-R	5′-GCAACCATTCGTCGTTGGCAACAAGC-3′
RmMDH-F	5′- TCCCATTTTCCACCTTTCAGATC-3′
RmMDH-R	5′- CCATCATTACCCGTCGACTCAAG -3′
EF-1α-F	5'- TGTCATCGATGCTCCTGGAC -3'
EF-1α-R	5'- TCTCGGGTCTGACCATCCTT -3'
CYP -F	5'- AGGGCCGAAATGTCGTTCTA -3'
CYP -R	5'- CCCATCTCCAGCCAAATCAT -3'
Q-*RmMDH*-F	5'- TGAGGCACTGAATGGAGTGAAA -3'
Q-*RmMDH*-R	5'- CTTTCCTAGGGAACCCACCAAC -3'
RmMDH-F′	5′-CGCGGATCCTTCAGTTTTACCTCTCTG-3′, *Bam*HI site underlined
RmMDH-R′	5′-GCGGTCGACATTCAAAGGAGAGGAGGG-3′, *Sal*I site underlined

Bioinformatics analysis of *RmMDH*: The generated sequence was verified for similarity using the BLAST program (http://blast.ncbi.nlm.nih.gov/). When ORF finder (http://www.ncbi.nlm.nih.gov/gorf/gorf.html) was utilized to obtain ORF, we adopted DNAMAN to translate coding sequence (CDS) to amino acid sequence. Protparam (http://web.expasy.org/protparam) was employed to analyze those estimated proteins for their physiochemical characters. Hydrophobic analysis of RmMDH was carried out using ProtScale (https://web. expasy. org/protscale/). Protein phosphorylation sites were predicted using tools at the NetPhos 3.1 server (http://www.cbs.dtu.dk/services/NetPhos/). NetNGlyc 1.0 (http://www.cbs.dtu.dk/Services/NetNGlyc/) was utilized to predict N-glycosylation sites. The Cell-PLoc 2.0 online approach (http://www.csbio.sjtu.edu.cn/bioinf/plant-multi/) was employed to predict subcellular localization. NPSA (https://npsa-prabi.ibcp.fr/cgi-bin/npsa_automat.pl?page=/ NPSA/npsa_seccons.html) was used to predict secondary structure, and the three-dimensional (3D) structure was obtained using tools at the SWISSMODEL server (https://swissmodel.expasy.org/). The conserved domains of *RmMDH* were analyzed using tools at the NCBI Conserved Domain Database (https://www.ncbi.nlm.nih.gov/Structure/cdd/wrpsb.cgi). DNAMAN version 9 was adopted for multiple sequence alignment, while MEGA X was utilized to construct a phylogenetic tree via neighbor-joining under 1000 bootstraps.

Quantitative real-time PCR analysis of *RmMDH*: For investigating *RmMDH* expression profiles within *Rh. micranthum*, this study isolated total RNAs from flower, leaf, stem and root samples, respectively, according to the identical method adopted in section 2.2. Thereafter, PrimeScript RT reagent kit was utilized to purify RNA

and synthesize first-strand cDNA by using gDNA Eraser (Takara), and the cDNA was diluted 10-fold before use. Previous studies have shown that *EF-1α* is the most stable reference gene among different tissues (leaves, roots, stems, and flowers) at the same developmental stage, while *CYP* is the most stable reference gene among flowers at different developmental stages (Schulze *et al*., 2002a; Scheibe 2004; Schulze *et al*., 2002b). Therefore, these genes were used as internal reference genes as appropriate. Table 1 lists all primers adopted in qRT-PCR. The 20 μL qRT-PCR system contained 50×ROX Reference Dye II (0.4 μL), 2×SYBR Premix Ex Taq™ (10 μL, Takara), forward and reverse primer (each 0.4 μL, 10 μM), ddH_2O (6.8 μL) and diluted cDNA (2 μL, 200 ng). Each reaction was carried out thrice. The ABI GeneAmp PCR 9700 thermal cycler (ABI, Foster City, CA, USA) was employed for qRT-PCR by the two-step process, including 30 s under 95°C; followed by 5 s under 95°C and 34 s under 60°C for 40 cycles. Subsequently, this study conducted melting curve analysis by the following process, 15 s under 95°C, 60 s under 60°C and 15 s under 95°C. The standard curve was calibrated by serial cDNA dilution for every gene, so as to guarantee the almost identical target and reference gene primer amplification efficiency (about 100%). The $2^{-\Delta\Delta Ct}$ approach (Livak & Schmittgen, 2001) was utilized to calculate relative *RmMDH* transcript expression.

Southern blot analysis: The integration of *RmMDH* to tobacco genome was confirmed by Southern blot hybridization assay, which was also applied in estimating the copy number of transgene. The CTAB protocols were adopted to prepare genomic DNA based on tobacco leaf samples. To carry out Southern blotting assay, about 20 μg genomic DNA was isolated from every line for *Bam*HI digestion. Thereafter, the digoxigenin (DIG)-High Prime DNA Labeling and Detection Starter Kit I (Mylab Medical Technology, Beijing, China) was utilized for Southern blotting hybridization assay in line with specific protocols.

Construction of overexpression vector and genetic transformation into tobacco: Gene-specific primers *RmMDH*- R′ and *RmMDH*-F′ were utilized to amplify *RmMDH* ORF (Table 1), followed by cloning of amplified product to the pBI121 expression vector harboring the CaMV35S promoter. Subsequently, the pBI121-*RmMDH* vector was transferred into the *Agrobacterium tumefaciens* strain GV3101, which was cultured to a suitable concentration. Using the leaf disc transformation method, transgenic (TM) tobacco plants were generated. Then, we selected seeds from TM plants in the MS medium that contained kanamycin (100 $mg \cdot L^{-1}$). Thereafter, this study transferred the T2 positive plants into the substrate mixture that contained peat, perlite and vermiculite (3:0.5:1, v/v). Later, qRT-PCR was conducted to confirm that transgene was harbored in the surviving transformants.

Growth phenotypes and physiological indexes of transgenic tobacco plants: We sowed seeds from homozygous TM plants as well as the relevant wild-type (WT) plants in the MS medium (that contained 0.8% agar and 30 g/L sucrose). At 10–12 days later, we transferred each seedling into corresponding pot that contained equivalent substrate mixture in weight. The plant height, leaf width, leaf length, and leaf area were recorded 45 days after the seedlings were transplanted.

Thereafter, we grew TM plants in the MS medium that contained kanamycin (50 $mg \cdot L^{-1}$), whereas WT lines in the kanamycin-free MS medium. The growth conditions were as follows: 25°C, 16-h light/8-h dark photoperiod. After 30 days of growth, the TM plants showed resistance and sensitivity separation. The bud tip tissue (about 1 cm) of resistant plants was cut and inoculated onto MS medium containing 200 mM NaCl, 5% (w/v) polyethylene glycol (PEG) 6000, 50 μM $AlCl_3$, or 20 mM $NaHCO_3$, and grown for 7 days. All stress treatments were completed under otherwise consistent growth conditions. This study harvested the first tender leaves of seedlings and freeze them into the liquid nitrogen at once for the analysis of free proline levels depicted by Bates (Bates *et al*., 1973) and malondialdehyde (MDA) levels (an index of lipid peroxidation) using a spectrophotometric method as described by Hodges (Hodges *et al*., 1999).

Data processing and analysis: SPSS17.0 (Chicago, IL, USA) was employed to statistically analyze relative expression of gene transcripts. After calculating averages and standard errors (mean ± SE) for each sampling time, significance of difference in each growth index was detected between WT and TM groups by *t* test. Differences in physiological indexes between TM and WT plants were assessed by post-hoc Duncan's multiple range tests and one-way ANOVA.

Results

Identification and phylogenetic analysis of *RmMDH* in *Rh. Micranthum*: This work extracted *RmMDH* full-length cDNA sequence based on *Rh. Micranthum* leaf samples (Supplementary file 1, Fig. S1). The *RmMDH* open reading frame (ORF) and protein sequences were predicted and compared (Fig. 1A). Analyses using ProtParam showed that the ORF of *RmMDH* was 999 bp, which was also responsible for encoding a protein that contained 332 amino acids, its estimated molecular mass was 35.61 dDa whereas its theoretical isoelectric point was 6.40. The instability index was calculated to be 35.78, which classified the protein as stable. The grand average of hydropathicity (GRAVY) value was 0.069. BlastP and conserved domain searches in the NCBI database revealed that *RmMDH* belongs to the MDH family. In comparative analyses, the amino acid sequence of *RmMDH* showed high similarities with homologs in other plants. Conserved domain analyses showed that RmMDH contains classical NAD-binding and carboxy C-terminal domains (Fig. 1B). Phylogenetic tree constructed according to MDH protein nucleotide coding sequences was divided into three major subgroups; typically, amino acid sequence of RmMDH shared the greatest identity (91%) to MDH isolated from *Camellia oleifera* (ANN22405.1) (Fig. 1C).

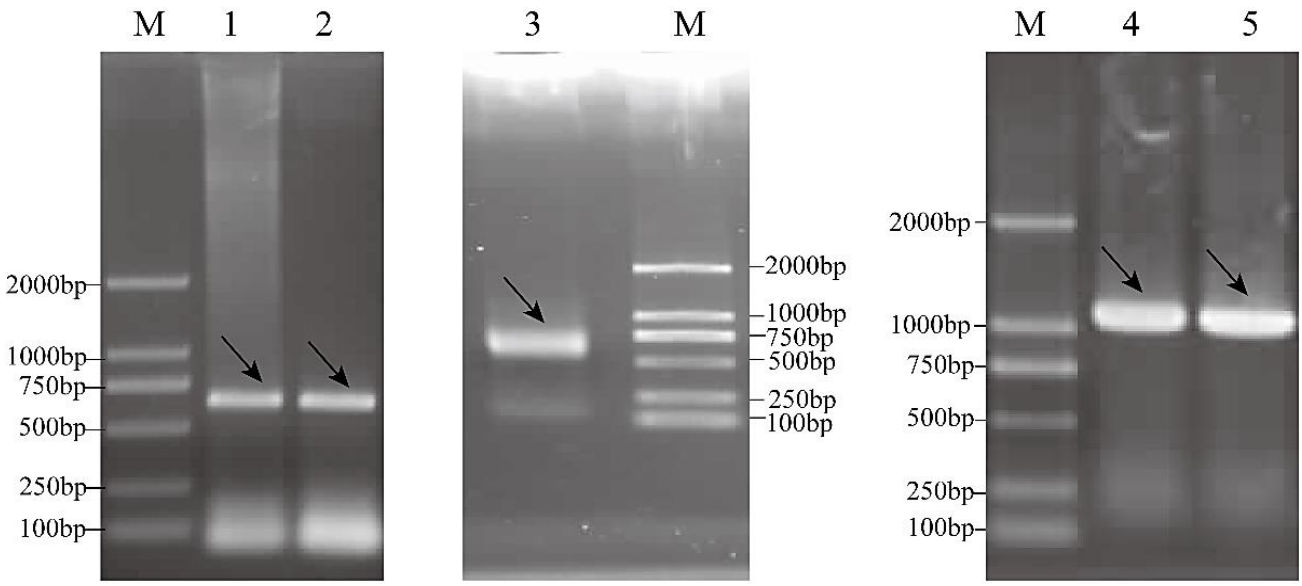

Fig. S1. The PCR amplification product of the *RmMDH*. M: DL 2000 marker; 1, 2: The PCR product of 3'RACE cDNA. 3: The PCR product of 3'RACE cDNA. 4, 5: The PCR product of full-length cDNA.

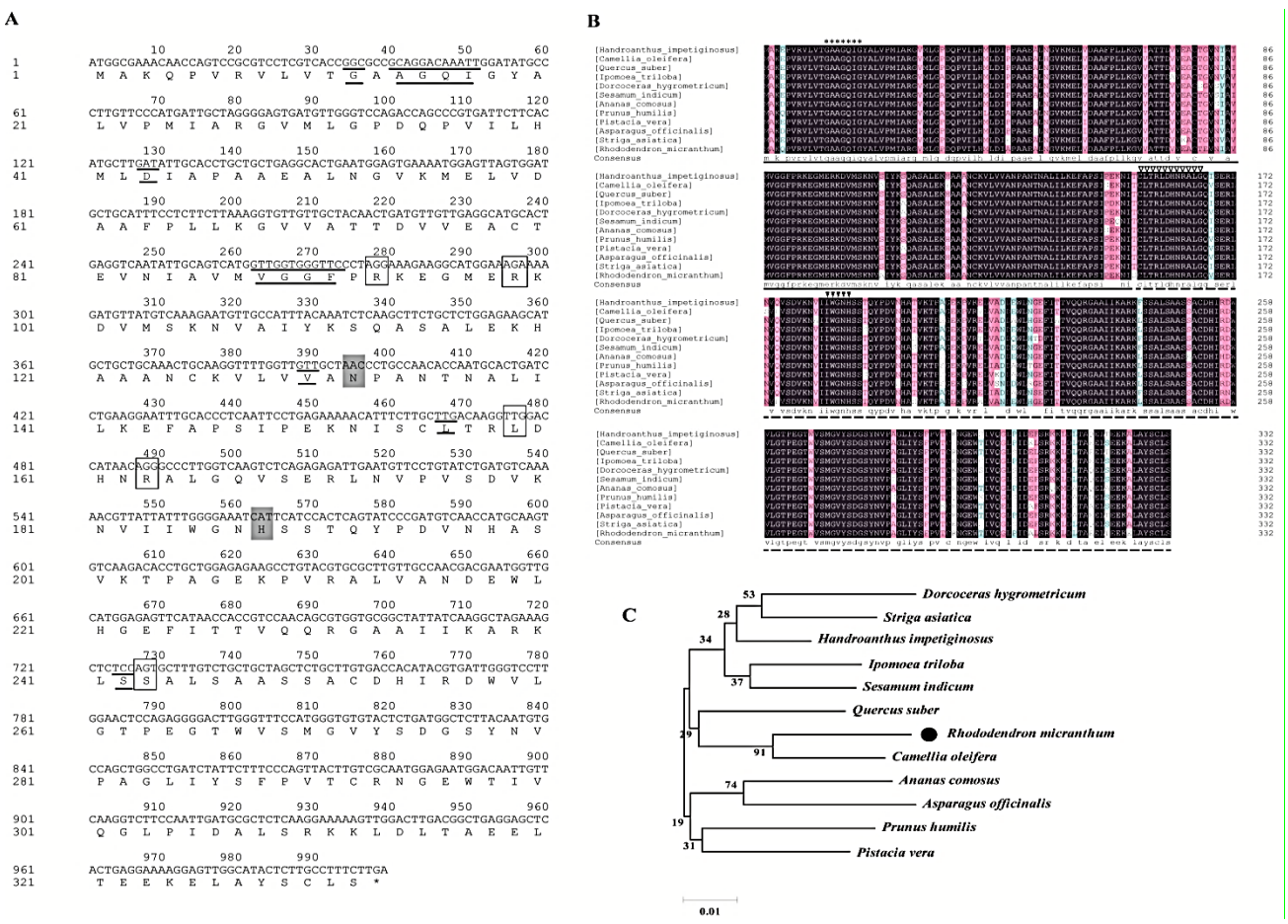

Fig. 1. *RmMDH* nucleotide sequence and RmMDH deduced amino acid sequence (A), alignment of multiple sequences (B), and phylogenetic associations among the chosen MDH proteins (C). (a) *RmMDH* open reading frame (upper panel) and deduced amino acid sequence (lower panel). Start codon is ATG and stop codon (TGA) is marked with an asterisk. Box indicates MDH binding site, NAD binding site is underlined, shading indicates dimer binding site. (b) RmMDH and other MDH protein amino acid sequence alignment. Broken and solid lines under the sequence stand for carboxy C-terminal and NAD-binding domains, separately. Hollow triangles indicate MDH active site, solid triangles stand for catalytic group, whereas asterisks indicate glycine motif. GenBank accession numbers of RmMDH and other MDH sequences are as follows: *Handroanthus impetiginosus* (PIN14152.1), *Camellia oleifera* (ANN22405.1), *Quercus suber* (XP_023879128.1), *Ipomoea triloba* (XP_031098474.1), *Dorcoceras hygrometricum* (KZV43577.1), *Sesamum indicum* (XP_011091314.1), *Ananas comosus* (XP_020094482.1), *Prunus humilis* (ALI57374.1), *Pistacia vera* (XP_031252906.1), *Asparagus officinalis* (XP_020250168.1), *Striga asiatica* (GER52265.1), *R. micranthum* (AFI08586.1). (c) Neighbor-joining tree constructed using bootstrap method.

RmMDH hydrophobicity and hydrophilicity were analyzed through ProtScale, while Doolittle & Hphob./Kyte were chosen to be the standards for prediction. In the polypeptide chain, the highest score of 1.978 at the position 41 Met (M) stood for the greatest hydrophobicity, whereas the smallest score (−2.867) at the position 97 Met (M) represented maximal hydrophilicity (Supplementary file 1, Fig. S2A). Hydrophobic residues were detected in altogether 259 amino acid sequences; as a result, we suggested that the mean hydrophobicity index of the whole polypeptide chain was 0.062. Such finding conformed to those obtained from ProtParam analysis, indicating that RmMDH is a hydrophobic protein. N-glycosylation sites in RmMDH were predicted using NetNGlyc 1.0, as shown in (Fig. S3A) a potential N-glycosylation site was detected at Ser-187 (probability, 0.6169). Further analysis of the deduced amino acid sequence using NetPhos 3.1 revealed 38 potential phosphorylation sites, including 13 serines (Ser), 11 threonines (Thr), and four tyrosines (Tyr), at the threshold of 0.5 (Supplementary file 1, Fig. S3B). N-glycosylation accounts for an important modification following eukaryotic protein translation, which has certain effect on protein charge and thermostability.

Secondary structure analysis revealed that RmMDH consists of α-helixes (45.18%), extended strands (17.47%), and random coils (33.13%) (Fig. 2B). Conserved domain predictions showed that RmMDH belongs to the MDH family (Fig. 2C). To investigate the 3D structure of RmMDH, SWISS-MODEL was adopted to analyze the amino acid sequence. Based on homology modeling and threading, a RmMDH protein 3D model was constructed (Supplementary file 1, Fig. S4A). Analyses using Cell-PLoc 2.0 predicted that RmMDH is localized to the chloroplast (Supplementary file 1, Fig. S4B).

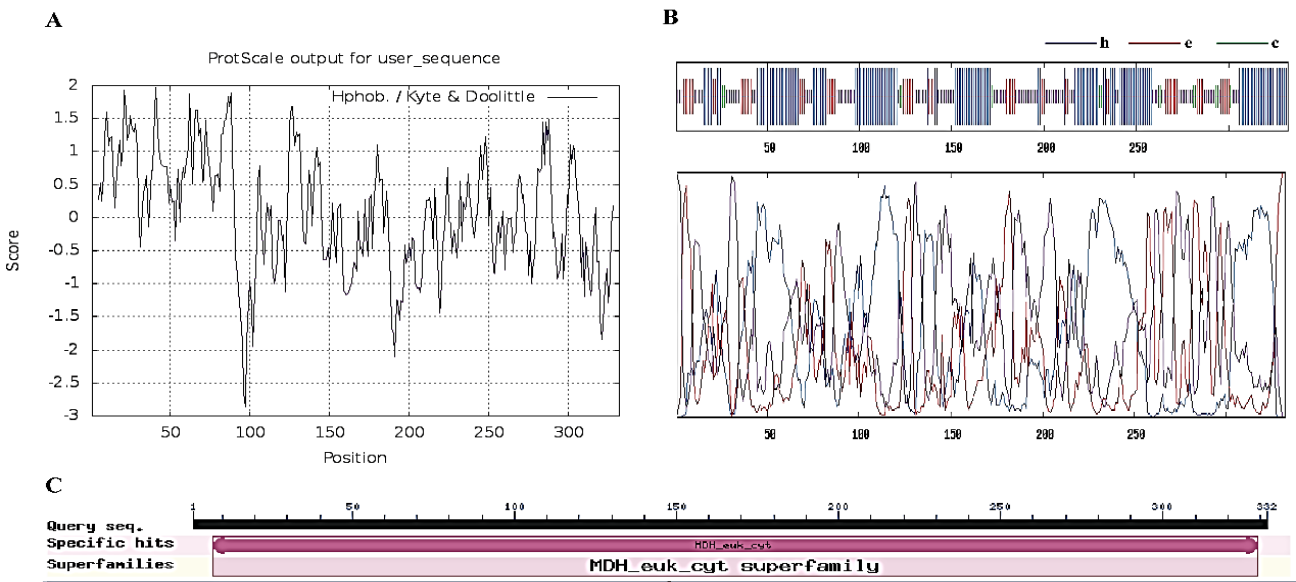

Fig. S2. RmMDH hydrophobicity profile analysis (A), secondary structure (B) and domain prediction(C). (b) letter ‘h’, ‘e’, and ‘c’ are represented α-helix, extended strand and random coil, respectively.

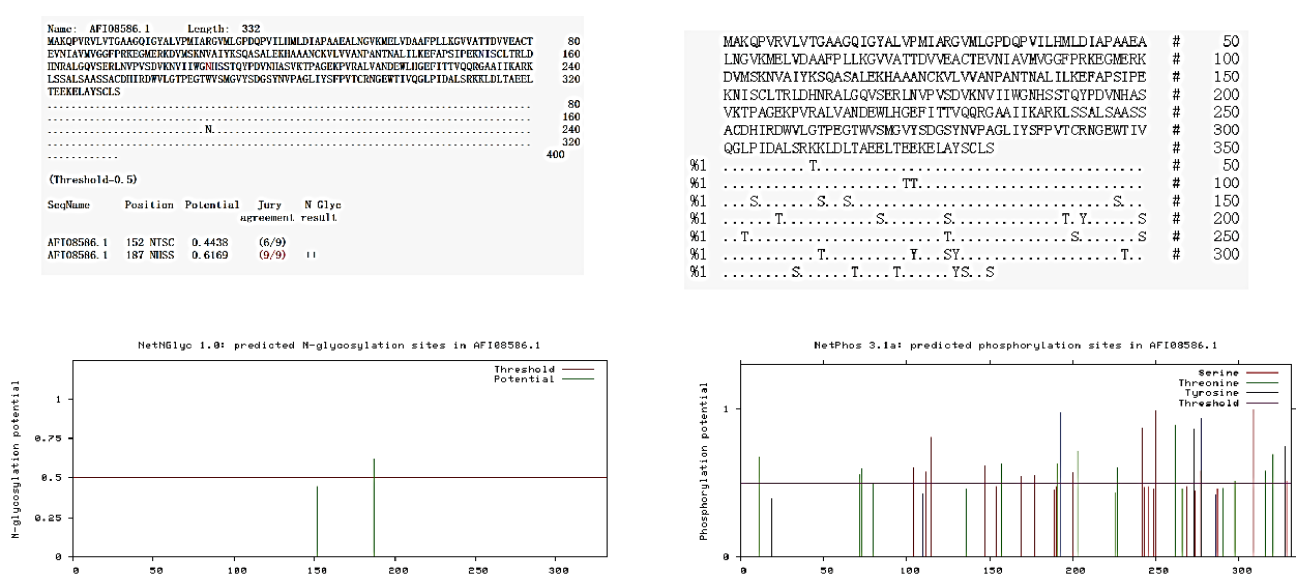

Fig. S3. Prediction of potential phosphorylation sites and N-glycosylation sites of RmMDH. (a) Prediction of phosphorylation sites of RmMDH. (b) Prediction of N-glycosylation sites of RmMDH.

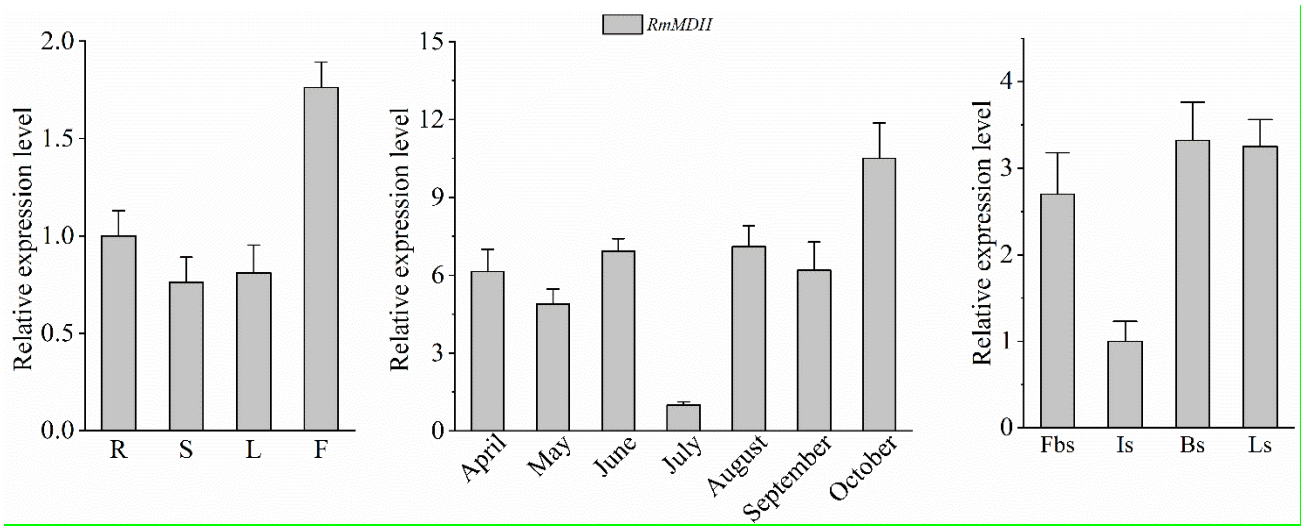

Fig. 2. Transcript levels of *RmMDH* in different tissues (A) and at different developmental stages in flowers (B) and leaves (C) as detected by qRT-PCR. R, S, L, F indicate roots, stems, leaves, and flowers, respectively. Bds, Ifs, Fbs, Lfs indicate flower bud differentiation stage, initial flowering stage, full-bloom stage, and last flowering stage, respectively. Means±SD were determined based on 3 duplicates. The diverse lower-case letters stand for statistical significance (p<0.05 by Duncan's test).

A

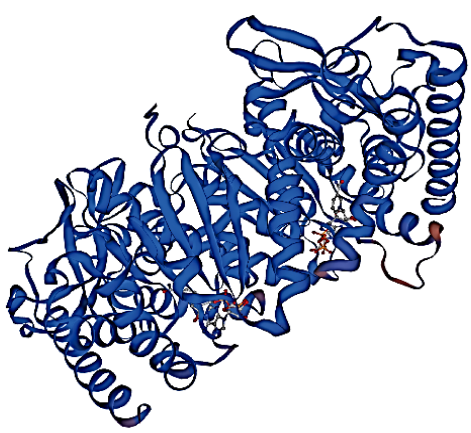

B

Plant-mPLoc:Predicting subcellular localization of plant proteins including those with multiple sites

| Read Me | Data | Citation |

Your input sequence (332aa) is:

>AFI08586.1 malate dehydrogenase [Rhododendron micranthum]
MAKQPVRVLVTGAAGQIGYALVPMIARGVMLGPDQPVILHMLDIAPAAEALNGVKMELVD
AAFPLLKGVVATTDVVEACTEVNIAVMVGGFPRKEGMERKDVMSKNVAIYKSQASALEKH
AAANCKVLVVANPANTNALILKEFAPSIPEKNISCLTRLDHNRALGQVSERLNVPVSDVK
NVIIWGNHSSTQYPDVNHASVKTPAGEKPVRALVANDEWLHGEFITTVQQRGAAIIKARK
LSSALSAASSACDHIRDWVLGTPEGTWVSMGVYSDGSYNVPAGLIYSFPVTCRNGEWTIV
QGLPIDALSRKKLDLTAEELTEEKELAYSCLS

---------- Plant-mPLoc Computation Result ----------

Query protein	Predicted location(s)
AFI08586.1 malate dehydrogenase [Rhododendron micranthum]	**Chloroplast.**

Fig. S4. Three-dimensional (3D) structure model and subcellular localization prediction of RmMDH protein. (a) RmMDH 3D structure displayed in solid ribbon style; (b) subcellular localization prediction of RmMDH.

Transcript levels of *RmMDH* in different tissues of *Rh. Micranthum*: We detected *RmMDH* transcripts in the roots, stems, leaves, and flowers, but the levels differed significantly among these tissues. The transcript levels of *RmMDH* in different tissues were normalized against that of *EF-1α*. Flowers showed the greatest *RmMDH* transcript expression, followed by that in leaf, stem and root samples. The transcript level in the flowers was 1.76-fold that in the roots, and the transcript level in the stems was 0.81-fold that the roots (Fig. 2).

The transcript levels of *RmMDH* in flowers differed among different developmental stages (Fig. 2). In these analyses, the transcript level of *RmMDH* was normalized against that of *CYP*. The transcript levels of *RmMDH* were higher at the full-blooming stage (Fbs) than at the last flowering stage (Lfs), and were lowest at the initial flowering stage (Ifs) (Fig. 2). The transcript levels of *RmMDH* at the Fbs and Lfs were, respectively, 3.32-fold and 3.25-fold that at the Ifs. The transcript level of *RmMDH* was 2.7-fold higher at the Fbs than at the flower bud differentiation stage (Bds). The above results suggested the potentially vital function of *RmMDH* in reproductive organs of *R. micranthum*, especially during the Fbs stage.

Southern blot and PCR analysis: The copy number of *RmMDH* cDNAs integrated into the tobacco host genome was determined by Southern blot analysis. Genomic DNA was extracted from three TM lines and WT plants using the CTAB method and digested with *Bam*HI. Wild-type (WT) tobacco and the pBI-121 plasmid were used as the negative and positive control, respectively. Two transgenic lines TM2 and TM3 had single bands confirming integration of a single copy of the transgene into the tobacco genome (Fig. 3), while WT plants had no hybridization signals. These results confirmed integration of *RmMDH* into the genome of the TM lines. We also detected successful integration of *RmMDH* into the genome of genetically modified *Rh. micranthum* overexpressing *RmMDH* in the leaves (Supplementary file 1, Fig. S5).

Ectopic expression of *RmMDH* inhibits growth of transgenic tobacco plants: The plant height differed significantly between TM and WT tobacco lines (Fig. 4). The average plant height of TM1, TM2, and TM3 was 62.29 cm, 65.36 cm, and 67.28 cm, respectively, lower than that of WT (83.38 cm) (Fig. 5). The leaves of the TM lines were smaller than those of WT (Fig. 4). The average leaf area of WT was 97.71 cm^2, and those of the TM lines were decreased by 16.59%–42.9% (Fig. 5). Therefore, TM plants were deemed as homozygous and adopted for later experiments.

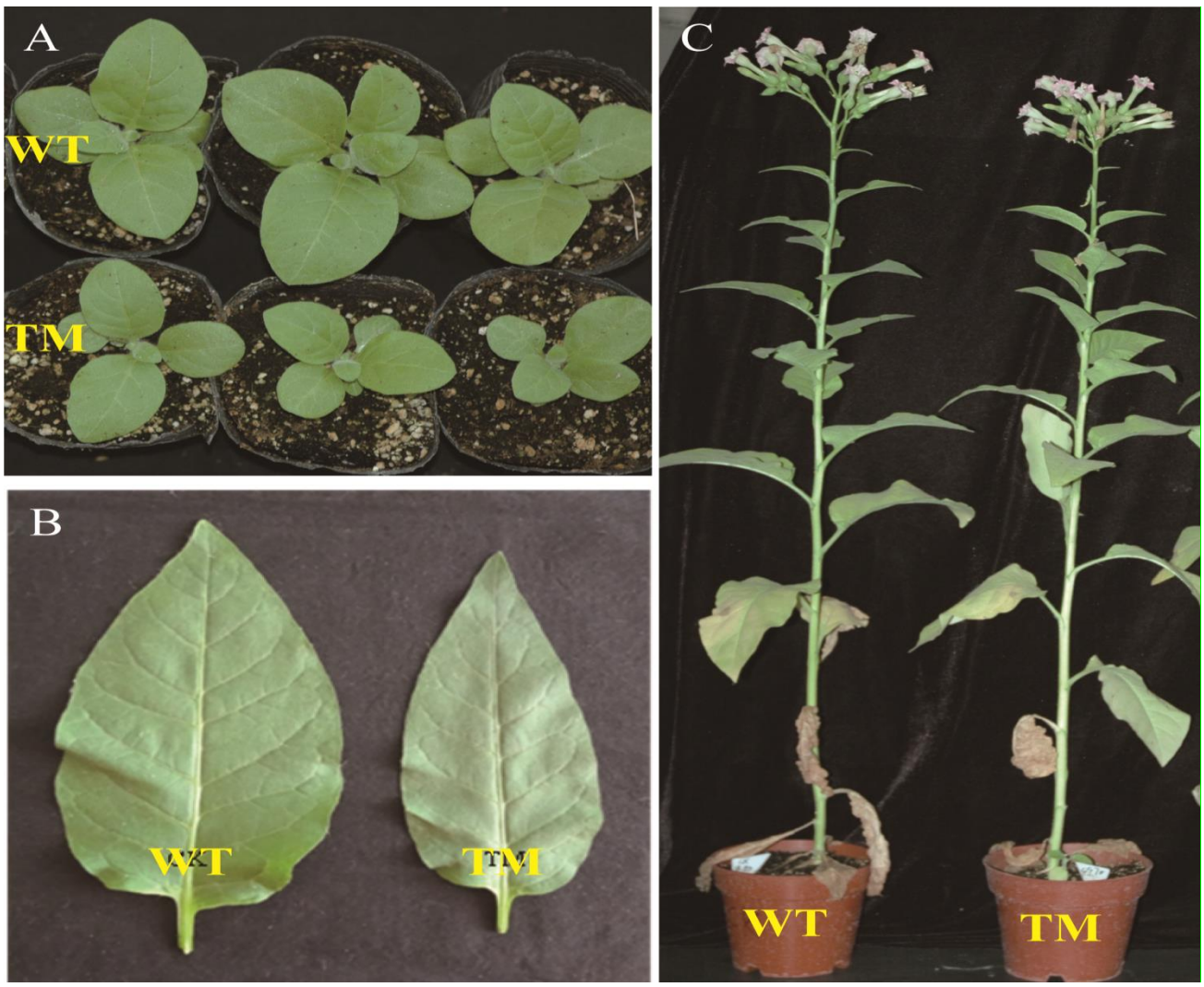

Fig. 4. Morphological features of wild-type and transgenic tobacco plants overexpressing *RmMDH*.

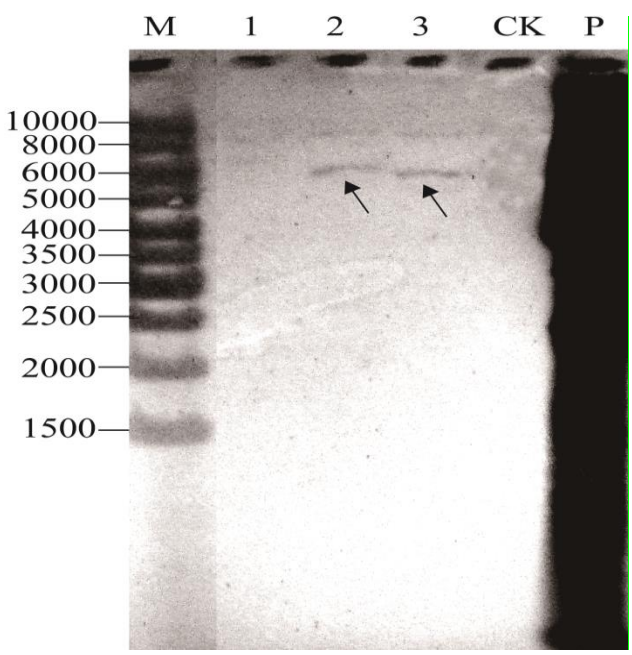

Fig. 3. Southern blotting analysis of *RmMDH*. M: 10,000 bp DNA marker; Lane 1, Lane 2: Negative controls; Lane 3, Lane 4: Positive lines; CK: Non-transgenic tobacco lines, P: Plasmid DNA. Black arrows indicate target bands.

Ectopic expression of *RmMDH* reduces MDA and proline accumulation in transgenic tobacco: Transgenic tobacco plants were treated with NaCl, PEG, and $AlCl_3$, and the MDA and proline contents were determined after 7 days of exposure to these stresses. MDA level represents a lipid peroxidation indicator. The MDA contents of TM1, TM2, and TM3 were similar among the three stress treatments. MDA level markedly decreased in TM plants compared with WT with each stress treatment (Fig. 6A). In the NaCl treatment, the MDA content in TM1, TM2, and TM3 was 58.34%, 66.58% and 58.68% of that in WT, respectively. In the $NaHCO_3$ treatment, the MDA content in TM1, TM2, and TM3 was 48.81%, 50.4%, and 58.36% of that in WT, respectively. In the PEG treatment, the MDA content in TM1, TM2, and TM3 was 72.24%, 75.95%, and 84.59% of that in WT, respectively. In the $AlCl_3$ treatment, the MDA content in TM1, TM2, and TM3 was 39.54%, 49.18%, and 50.18% of that WT, respectively.

The proline concentration in plants usually increases under stress conditions, and this provides protection against abiotic stresses. In this study, the proline levels markedly increased in those 3 TM lines compared with WT. The proline content in TM plants increased by 47%, 52.67%, 62% and 43%, respectively, compared with that in WT under saline, alkaline, drought and Al^{3+} stress conditions (Fig. 6B).

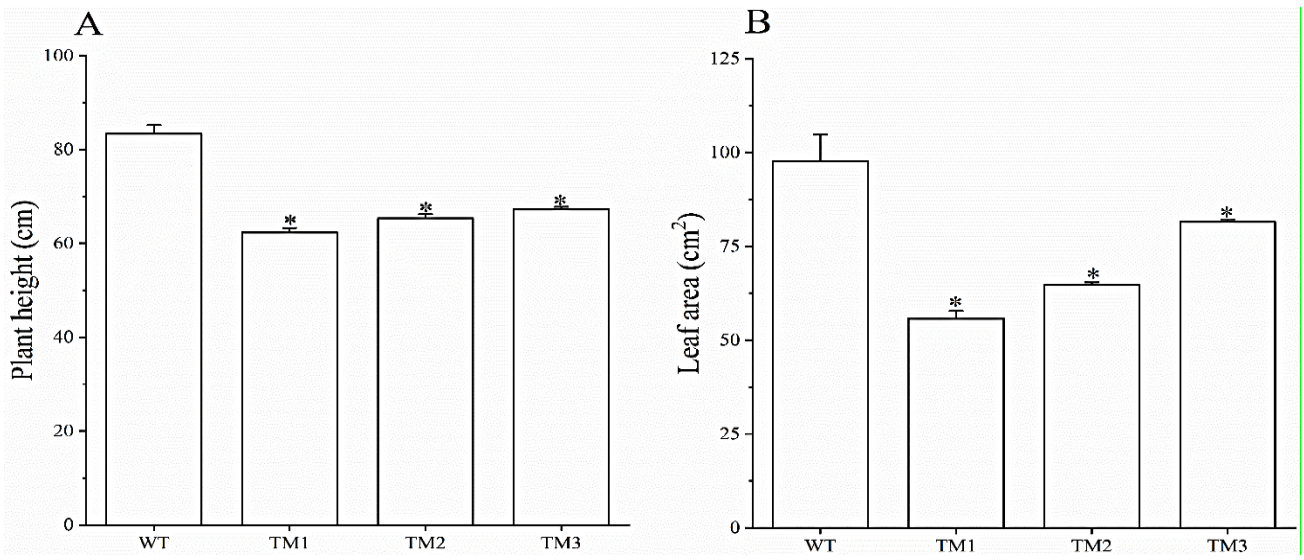

Fig. 5. Plant height (A) and leaf area (B) of transgenic and wild-type tobacco. Asterisks stand for statistical significance (p<0.05, t test).

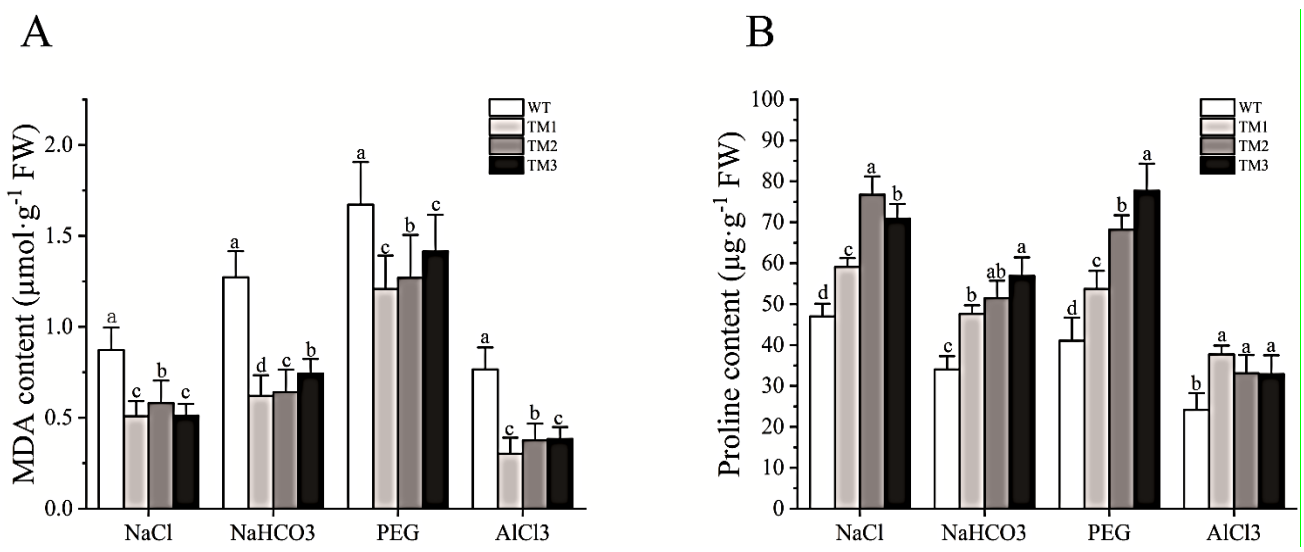

Fig. 6. MDA (A) and proline (B) levels within *RmMDH*-overexpressing transgenic and wild-type tobacco plants under abiotic stress treatments (NaCl, $NaHCO_3$, PEG and $AlCl_3$). Each value represents mean of three replicates. The diverse lower-case letters stand for statistical significance (p<0.05 by Duncan's test).

Fig. S5. Overexpression transgenic *R. micranthum* Turcz. tissue culture seedlings. A-C, *R. micranthum* Turcz. tissue culture seedlings at different growth stages; D, Rooting of *R. micranthum* Turcz. tissue culture seedlings; E, Electrophoresis gels of PCR products amplified from independent transgenic *R. micranthum* Turcz. (M: DL 2000 marker).

Discussion

Malate represents the vital intermediate involved in plant cell energy supply, metabolism and nutrition (Schulze *et al*., 2002b, 2002a). MDHs play vital parts in the generation of malate, which have attracted wide attention from scientists (Schulze *et al*., 2002a; Scheibe, 2004; Schulze *et al*., 2002b), and many researchers have studied their functions. Nonetheless, many relevant works are carried out on model plants (Gietl 1992; Pracharoenwattana *et al*., 2007; Tomaz *et al*., 2010; Selinski *et al*., 2014). It is still unknown about *MDH* genes' functions in ornamental plants.

In this study, an *MDH* gene designated as *RmMDH* was cloned from *Rh. micranthum*. Comparative analyses showed that it was tightly associated with *MDH* in *Camellia oleifera.* In addition, as revealed by qRT-PCR results, the *RmMDH* transcript levels differ among different tissues and among flowers and leaves at different stages of development. Therefore, our results show that *RmMDH* has a special spatiotemporal expression pattern.

Amino acid sequence analysis revealed that RmMDH has an NAD-binding site, a malic acid-binding site, and a dimer-binding site, like other members of the MDH family (Yao *et al*., 2008). In addition, RmMDH contains the NAD combined site 'GAAGQIG,' and the catalytic sequence 'IWGNH', both of which are the fundamental and highly-conserved components in diverse species (Jia *et al*., 2013; Muhammad *et al*., 2017). The predicted cellular localization of RmMDH is the chloroplast. Together, these results strongly indicate that RmMDH is a cytosolic MDH protein. Based on analysis results of secondary structure, RmMDH was mostly comprised of random coils and α-helixes, both of which were intertwined with extended strands and β-turns. Notably, random coil and bend structures have important functions in MDH reaction, since NAD-binding domain and catalytic site exist in the above domains.

Flower samples had the greatest *RmMDH* transcript expression level, such as *MDH* within banana (*Musa acuminata* L. AAA group). The *MaMDH* expression patterns in banana were found to correlate with ethylene biosynthesis (Jia *et al*., 2013). Roots had decreased *RmMDH* transcript level compared with stems, leaves, and flowers. Similarly, the transcript levels of cotton *GhcMDH1* were found to be high in leaf and stem samples relative to root samples (Muhammad *et al*., 2017). These results suggest that *RmMDH* possibly had certain physiological activities in the development of plants. We detected *RmMDH* transcripts in all tissues, suggesting that it may be a house-keeping gene.

In the transgenic tobacco plants, ectopic *RmMDH* expression suppressed plant growth while enhancing the resistance to Al^{3+} stress. Compared with WT plants, the TM lines were shorter and had a smaller leaf area. In contrast with our findings, previous studies reported that overexpression of *BraMDH* accelerated plant growth and development (Li *et al*., 2016), and overexpression of *GhmMDH1* increased the biomass and reduced the respiration rate within the transgenic cotton plants (Wang *et al*., 2015). However, other studies have reported similar results to ours. For example, transgenic *neMDH* alfalfa were smaller than wild-type plants when grown in soil under greenhouse conditions (Tesfaye *et al*., 2001). Such growth pattern might result from the restricted carbon availability, due to the exhaustion of carbon source since great quantities of organic acids were secreted, thus preventing physiological plant growth (Tesfaye *et al*., 2001). We can speculate that the reason for the increase in Al^{3+} resistance in transgenic tobacco overexpressing *RmMDH* may be increased conversion of oxaloacetic acid into organic acids like malate. This is supported by the results of previous studies, for example, certain plant species produce organic acids (like oxalate, malate, citric acid) in rhizosphere when exposed to Al^{3+} stress; as a result, the resultant organic acids and Al^{3+} produce the non-toxic complexes, thus preventing the penetration in roots (Ma *et al*., 2001; Kochian *et al*., 2004). In transgenic alfalfa, *NeMDH* over-expression improved Al^{3+} resistance and organic acid production (Tesfaye *et al*., 2001).

We found that overexpression of *RmMDH* increased tolerance to other abiotic stress, and resulted in increased proline content and lower MDA content. Generally, proline production increases in the case of osmotic stress, which stabilizes cellular redox status (Hare *et al*., 1999; Szabados & Savoure, 2010). These results are similar to those reported for transgenic tomato plants expressing cytosolic MDH (Wang *et al*., 2010), and maize plants overexpressing *ZmNADP-MDH* that showed decreased H_2O_2 and MDA production (Kandoi *et al*., 2018).

Conclusion

An *MDH* gene designated as *RmMDH* was isolated from *Rh. micranthum*. RmMDH was predicted to localize to the chloroplast. Phylogenetic analysis indicated that *RmMDH* shares 91% identity with MDH from *Camellia oleifera*. This study also measured *RmMDH* transcript levels within diverse tissues, and the greatest transcript expression was measured within flowers. The peak transcript levels of *RmMDH* in flowers were at the full blooming stage and the peak levels in leaves were in October. The transcript levels of *RmMDH* changed in response to Al stress and other abiotic treatments (NaCl, $NaHCO_3$, and PEG). Ectopic expression of *RmMDH* improved tolerance to Al^{3+} and three other abiotic stresses in transgenic tobacco, but also led to reduced plant height and leaf area, increased proline content, and decreased MDA content. This is the first report of the isolation, expression analysis, and preliminary functional characterization of *RmMDH* from *Rh. micranthum.* These results provide a foundation for producing stress-resistant *Rh. micranthum* by gene transfer. Further studies are required to clarify the roles of the different domains of RmMDH in stress responses, and to identify other functions of RmMDH.

Acknowledgments

The authors wish to thank the Institute of Institute of Botany, Chinese Academy of Sciences, Beijing, China, for providing necessary facilities during the course of investigation, and Jennifer Smith, PhD, from Liwen Bianji, Edanz Group China (www.liwenbianji.cn/ac), for editing the English text of a draft of this manuscript.

References

Abd, D., El-Moneim, R. Contreras, J. Silva-Navas, F.J. Gallego, A.M. Figueiras and C. Benito. 2015. On the consequences of aluminium stress in rye: repression of two mitochondrial malate dehydrogenase mRNAs. *Plant Biol.,* 17(1): 123-133.

Allen, G.C., M.A. Flores-Vergara, S. Krasynanski, S. Kumar and W.F. Thompson. 2006. A modified protocol for rapid DNA isolation from plant tissues using cetyltrimethylammonium bromide. *Nature Prot.,* 1(5): 2320.

Bates, L.S., R.P. Waldren and I.D. Teare. 1973. Rapid determination of free proline for water-stress studies. *Plant & Soil.*, 39(1): 205-207.

Beeler, S., H.C. Liu, M. Stadler, T. Schreier, S. Eicke, W.L. Lue, E. Truernit, S.C. Zeeman, J. Chen and O. Kotting. 2014. Plastidial NAD-dependent malate dehydrogenase is critical for embryo development and heterotrophic metabolism in Arabidopsis. *Plant Physiol.*, 164(3): 1175-1190.

Gietl, C. 1992. Malate dehydrogenase isoenzymes: cellular locations and role in the flow of metabolites between the cytoplasm and cell organelles. *Biochimica et Biophysica Acta.*, 1100(3): 217-234.

Hare, P.D., W.A. Cress and J. Van Staden. 1999. Proline synthesis and degradation: a model system for elucidating stress-related signal transduction. *J. Exp. Bot.*, 50(333): 413-434.

Hodges, D. Mark, John M. Delong and R. Forney and K. Prange. 1999. Improving the thiobarbituric acid-reactive-substances assay for estimating lipid peroxidation in plant tissues containing anthocyanin and other interfering compounds. *Planta,* 207(4): 604-611.

Jia, C.H., J.H. Liu, Z.Q. Jin, Q.J. Deng, J.B. Zhang and B.Y. Xu. 2013. Isolation, characterization, and expression analysis of the MaMDH gene in banana. *Hortscien.*, 48 (5): 614-619.

Kandoi, D., M. Sasmita and C.B. Tripathy. 2018. Overexpression of plastidic maize NADP-malate dehydrogenase (ZmNADP-MDH) in *Arabidopsis thaliana* confers tolerance to salt stress. *Protoplasma,* 255(2): 547-563.

Kochian, L.V., O.A. Hoekenga and M.A. Pineros. 2004. How do crop plants tolerate acid soils? mechanisms of aluminum tolerance and phosphorous efficiency. *Ann. Rev. Plant Biol.*, 55(1): 459-493.

Li, Q.F., J. Zhao, J. Zhang, Z.H. Dai and L.G. Zhang. 2016. Ectopic expression of the chinese cabbage malate dehydrogenase gene promotes growth and aluminum resistance in Arabidopsis. *Front. in Plant Sci.*, 7:1180. doi: 10.3389/fpls.2016.01180

Livak, K.J. and T.D. Schmittgen. 2001. Analysis of relative gene expression data using real-time quantitative PCR and the 2(-Delta Delta C(T)) Method. *Methods,* 25(4): 402-408.

Luo, X.Y., Y.B. Cui, W. Deng, D.M. Li and Y. Pei. 2004. Transgenic alfalfa plants overexpressing nodule-enhanced malate dehydrogenase enhances tolerance to aluminum toxicity. *Mol. Plant Breed.,* 2(5): 621-626.

Ma, J.F., R. Peter and D. Emmanuel. 2001. Aluminium tolerance in plants and the complexing role of organic acids. *Trends in Plant Sci.*, 6(6): 273-278.

Muhammad, I., B. Zhang, K. Tang and J. Liu. 2017. Molecular characterization of a cytosolic malate dehydrogenase gene (GhcMDH1) from cotton. *Chem. Res. Chin. Univer*., 33(1): 87-93.

Pracharoenwattana, I., J.E. Cornah and S.M. Smith. 2007. Arabidopsis peroxisomal malate dehydrogenase functions in β-oxidation but not in the glyoxylate cycle. *Plant J.*, 50(3): 381-390.

Rudrappa, T., K.J. Czymmek, P.W. Pare and H.P. Bais. 2008. Root-secreted malic acid recruits beneficial soil bacteria. *Plant Physiol.*, 148(3): 1547-1556.

Scheibe, R. 2004. Malate valves to balance cellular energy supply. *Physiol. Plant.,* 120(1): 21-26. doi:10.1111/j.0031-9317.2004.0222.x.

Schulze, J., M. Tesfaye, R. Litjens, B. Bucciarelli, G. Trepp, S. Miller, D. Samac, D. Allan and C.P. Vance. 2002a. *Malate plays a central role in plant nutrition*: Springer Netherlands.

Schulze, J., M. Tesfaye, R. Litjens, B. Bucciarelli, G. Trepp, S. Miller, D. Samac, D. Allan and C.P. Vance. 2002b. Malate plays a central role in plant nutrition. *Plant & Soil*, 247(1): 133-139.

Selinski, J., K. Nicolas, W. Benedikt, T.H. Guy, L. Vera, H.N. Ekkehard and S. Renate. 2014. The plastid-localized NAD-dependent malate dehydrogenase is crucial for energy homeostasis in developing Arabidopsis thaliana seeds. *Molec. Plant.*, 7(1): 170-186.

Szabados, L. and S. Arnould. 2010. Proline: a multifunctional amino acid. *Trends in Plant Sci.*, 15(2): 89-97.

Tesfaye, M., J.T. Stephen, L.A. Deborah, P.V. Carroll and A.S. Deborah. 2001. Overexpression of malate dehydrogenase in transgenic alfalfa enhances organic acid synthesis and confers tolerance to aluminum. *Plant Physiol.*, 127(4): 1836-1844.

Tomaz, T., B. Matthieu, P. Itsara, L. Pernilla, P.L. Chun, J.C. Adam, S. Elke, M.S. Steven, G. Per and A.H. Millar. 2010. Mitochondrial malate dehydrogenase lowers leaf respiration and alters photorespiration and plant growth in arabidopsis. *Plant Physiol.*, 154(3): 1143-1157.

Wang, Q., Z. Yue, Y. Qiong, L. Kunzhi, Y. Yongxiong and C. Limei. 2010. Overexpression of malate dehydrogenase in transgenic tobacco leaves: Enhanced malate synthesis and augmented Al-resistance. *Acta Physiol. Plant.*, 32(6): 1209-1220.

Wang, Z., L. Qing, G. Xiaoyang, Y. Chunlin, L. Xiaoli, Z. Anhong, X. Juanli, T. Yingchuan, X. Guixian and C. Xiaoying. 2015. The mitochondrial malate dehydrogenase 1 gene GhmMDH1 is involved in plant and root growth under phosphorus deficiency conditions in cotton. *Scientific Rep.*, 5(1): 10343-10343.

Yao, Y., H. Yujin, L.I. Ming, P. Mingli, Liu. Zhi and Z. Heng. 2008. Gene clone, expression and enzyme activity assay of a cytosolic malate dehydrogenase from apple fruits. *Acta Hort. Sin.*, 2(3): 307-313.

Yao, Y.X., D.L. Qing, Z. Heng, X.Y. Chun and H.J. Yu. 2011a. The functions of an apple cytosolic malate dehydrogenase gene in growth and tolerance to cold and salt stresses. *Plant Physiol. & Biochem.*, 49(3): 257-264.

Yao, Y.X., L. Ming, Z. Heng, XY. Chun and J.H. Yu. 2011b. Isolation and characterization of an apple cytosolic malate dehydrogenase gene reveal its function in malate synthesis. *J. Plant Physiol.*, 168(5): 474-480.

Zhang, B.Y., Z.J. Hou, G.C Wang and G. Peng**.** 2015. Identification, characterization and quantitative analysis of NAD-malate dehydrogenase from the marine rhodophyte *Pyropia haitanensis*. *Bot. Marina,* 58(4): 285-293.

Zhang. 2008. Characterization of malate dehydrogenase gene from and its transgenic tobacco's tolerance to aluminium toxicity. *Acta Hort. Sinica,* 35(12): 1751-1758.

(Received for publication 8 March 2021)